Single-photon double K-shell ionization of low-Z atoms

2010 J. Phys.: Conf. Ser. 212 012006

(http://iopscience.iop.org/1742-6596/212/1/012006)

Journal of Physics: Conference Series **212** (2010) 012006 doi:10.1088/1742-6596/212/1/012006

Single-photon double K-shell ionization of low-Z atoms

J Hoszowska[1], A S Kheifets[2], J-Cl Dousse[1], I Bray[3], W Cao[1], K Fennane[1], Y Kayser[1], M Kavčič[4], J Szlachetko[1] and M Szlachetko[1]

[1]Department of Physics, University of Fribourg, CH-1700 Fribourg, Switzerland
[2]Research School of Physical Sciences, Australian National University, ACT 0200 Canberra, Australia
[3]ARC Centre for Matter-Antimatter Studies, Curtin University, WA 6845 Perth, Australia
[4]J. Stefan Institute, SI-1001, Ljubljana, Slovenia

E-mail: joanna.hoszowska@unifr.ch

Abstract. The photon energy dependence of the double K-shell ionization of light atoms is reported. Experimental double-to-single photoionization cross section ratios for Mg, Al, Si and Ca were obtained from measurements of high-resolution x-ray emission spectra. The double photoionization (DPI) cross-sections for K-shell hollow atom production are compared to convergent close-coupling calculations (CCC) for neutral atoms and He-like ions. The relative importance of the initial-state and final-state electron-electron interactions to the K-shell DPI in many-electron atoms and two-electron ions is addressed. Physical mechanisms and scaling laws of the K-shell double photoionization are examined. A semiempirical universal scaling of the DPI cross sections with the effective nuclear charge for neutral atoms $2 \leq Z \leq 47$ is established.

1. Introduction

The double photoionization (DPI) process has been a subject of intensive research both on the experimental and theoretical side and is still attracting considerable attention [1–11]. Because the photon interacts with only one of the bound electrons, two-electron ejection resulting from single-photon absorption is driven solely by many-electron interactions. Electron correlation effects lie in the heart of understanding of atomic structure. Yet, their quantitative description is far from complete or satisfactory. In the quest for an exact theoretical treatment of electron correlations in many-body systems the investigation of the photon energy dependence of single-photon double ionization of atoms is of fundamental importance.

The K-shell DPI of neutral elements produces K-shell hollow atoms i.e., atoms with an empty innermost shell and outer shells occupied. Thanks to the high brilliance and energy-tunability of x-ray synchtrotron radiation sources, experiments on the photon energy dependence of the DPI in neutral atoms became feasible. However, due to the low probability ($\sim 10^{-2}$-10^{-6}) for creating double K-shell vacancies, experimental investigation of the K-shell DPI in neutral atoms is quite challenging [10–16]. We report on the photon energy dependence of the double K-shell ionization of Mg, Al, Si and Ca [17, 18] for a wide range of photon energies from the DPI threshold up and beyond the maximum of the double-to-single photoionization ratios P_{KK}. So far, experimental results for P_{KK} far beyond the broad maximum are only available for He [19]. The experimental double-to-single photoionization cross-section ratios are compared to

convergent close-coupling calculations (CCC) for neutral atoms [18] and their corresponding two-electron ion counterparts. The relative contribution of the initial-state correlations and final-state electron-electron interactions to the K-shell DPI is addressed. Universal scaling of the DPI cross sections and the double-to-single photoionization ratios with the effective nuclear charge for neutral atoms is examined.

2. Experimental method

Experiments were performed at two undulator beam lines ID21 and ID26 at the European Synchrotron Radiation Facility (ESRF), using monochromatic synchrotron radiation and the Fribourg von Hamos Bragg-type curved crystal x-ray spectrometer [20]. The experimental method was based on the measurements of the high-resolution hypersatellite x-ray spectra following the radiative decay of the K-shell double vacancy states. For the studied low-Z elements, the Kα_2^h hypersatellite (^{1}P$_1\rightarrow{}^1$S$_0$) was predominant, the spin-flip Kα_1^h transition (^{3}P$_1\rightarrow{}^1$S$_0$) being dipole forbidden in the LS coupling scheme. As for light elements the K hypersatellites are partly overlapping with the L-satellites of the Kβ transitions, the use of high-resolution was mandatory. The double-to-single photoionization cross section ratios P$_{KK}$ were derived from the relative intensities of the resolved hypersatellite Kα^h ($1s^{-2} \rightarrow 1s^{-1}2p^{-1}$) to the diagram K$\alpha$ ($1s^{-1} \rightarrow 2p^{-1}$) x-ray transitions using the expression $P_{KK}=\frac{I_{K\alpha^h}}{I_{K\alpha}}\frac{\omega_K}{\omega_{KK}}$, where ω_K and ω_{KK} are the fluorescence yields for the single- and double- hole states [21], respectively. The DPI cross sections were determined employing the relation $\sigma^{2+} = P_{KK}\sigma^+$, where σ^+ stands for the single K-shell photoionization cross section from [22]. The Kα^h and Kα x-ray transitions were measured at different incident beam energies from 2.746 to 8.0 keV for Mg, from 3.122 to 7.0 keV for Al, from 3.6 to 10.0 keV for Si and for Ca in the 8.5 to 28.0 keV photon energy range. The intensities were corrected for sample self-absorption and absorption of the incident x-rays, the photon flux, the spectrometer solid angle, as well as for the detector quantum efficiency. The energy resolution of the spectrometer was comparable to the natural line widths of the measured K x-ray transitions. The incident photon flux was $\sim$1-3$\times10^{12}$ ph/s at both beam lines.

3. Theoretical model

The single and double photoionization cross sections were calculated using the convergent close-coupling (CCC) method. In the CCC formalism, the DPI is treated as a two step process. The first is the full absorption of the photon energy by one electron. The second is the interaction of this electron with the nucleus and the remaining electron which results in the promotion of the remaining electron into the continuum. To describe the first step, the 20-term Hylleraas ground state wave-function due to Hart and Herzberg [23] was employed for Mg^{10+}. For Al^{11+} and Si^{12+} more accurate results were obtained with a 9-term multi-configuration Hartree-Fock (HF) ground state calculated using the computer code by Dyall *et al.* [24]. The final states with two electrons in the continuum were described by a close-coupling expansion on the basis of channel functions. Calculations in the three gauges of the electromagnetic operator produced convergent results. More information on the photoionization CCC formalism can be found in Refs. [25, 26].

For neutral atomic targets Mg and Ca the CCC calculations of the K-shell DPI were based on the frozen-core model with two active ns^2 electrons which was used previously for the valence shell DPI [27]. Different ground-state wave functions of various degrees of correlation were used. Results of these new *ab initio* nonperturbative calculations for many-electron systems, including gauge convergence issues and difficulties, are reported by Kheifets *et al.* [18]. In the present paper, we compare the experimental data with the CCC calculations performed in the velocity gauge using the Hartree-Fock ground-state wave functions. These results were found to be closest to the experimental ones.

4. Results and Discussion

4.1. Double-to-single photoionization cross-section ratios

Single-photon double ionization is discussed in terms of two dominant mechanisms, namely, *shakeoff* (SO) and *knockout* (KO) [2–4, 9, 11, 28, 29]. Shake-off corresponds to a sudden ejection of the photoelectron following the single photon absorption and a subsequent change of the atomic field which may lead to a removal of the remaining electron to the continuum. To date, the shakeoff process is well defined in the asymptotic high-energy limit, but at finite energies no unique definition exists [30]. Despite this fact, the different SO expressions lead to quite similar numerical results. In case of KO, the outgoing photoelectron knocks out the second 1s electron in an (e,2e)-like electron impact half-collision. Initial ground-state correlations are important in SO, while final-state electron interactions govern KO. Although the two mechanisms have different interaction times and very different photon energy dependences, the separation of KO and SO with photon energy and the quantification of inteferences is not straightforward.

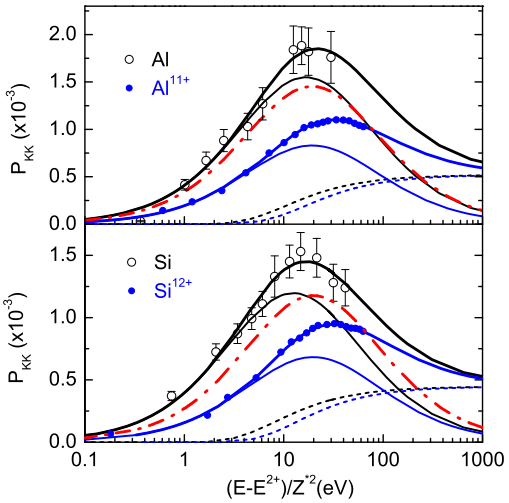

Figure 1. Double-to-single K-shell photoionization ratios for neutral atoms (black open circles) compared to the CCC calculations (velocity gauge) for the corresponding He-like ions (blue closed circles) as a function of the scaled excess energy. The best fits to our data (see text) are represented by solid thick lines, the KO by thin solid lines, and the SO by dashed lines. Black and blue lines correspond to the neutral atoms and ions, respectively. Red dot-dashed lines show the KO curve for the He-like ions scaled by Z^4/Z^{*4}.

To bring new insights as to the role played by outer shell electrons in the K-shell DPI, the phototoionization cross-sections for hollow atom production are compared to the CCC results of their corresponding two-electron ion counterparts. The experimental P_{KK}^{max} values for neutral atoms were found in good agreement with the $1/Z^{1.6}$-dependence suggested by Kanter *et al.* [10, 12] but systematically higher with respect to those of the He-like like ions. Because the influence of passive electrons on the ground-state correlations is small [31], one can assume that the photoabsorption asymptotic SO values for both neutral atoms and He-like ions are almost the same. Thus, the observed higher values of P_{KK}^{max} suggest that the electron scattering contribution to DPI is more important for neutral atoms compared to the He isoelectronic series. A clue to this finding resides in the proportionality of electron-impact ionization of a H-like ion to the KO term of the double photoionization of the corresponding He-like ion [3, 4, 28, 29]. Since along the hydrogen isoelectronic sequence the ionization cross sections σ_e scaled with the square of the ionization potentials I and plotted against the normalized electron energy E_e/I yield a universal curve [32], the KO contribution should scale with the square of the ionization potentials for a He-like ion and for the same neutral atom, respectively.

To corroborate the above statement, we have fitted the double-to-single K-shell ionization ratios for neutral and two-electron targets adopting an approach based on an incoherent summation of SO and KO terms. For $P_{KK}^{SO}(E)$ we have used the SO expression of Thomas [33] and for $P_{KK}^{KO}(E)$ the analytical form of the universal shape function for electron impact ionization of H-like ions of Aichele *et al.* given by Eq. (5) in Ref. [32]. The second ionization

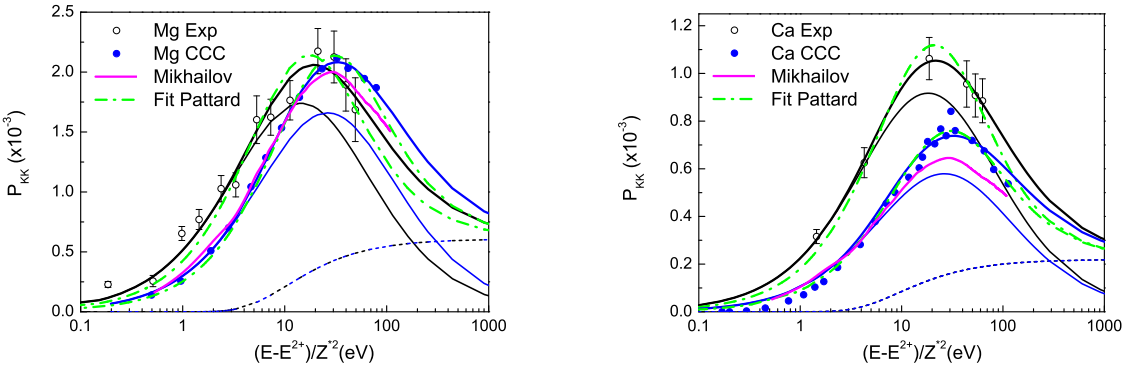

Figure 2. Double-to-single photoionization cross-section ratio of Mg and Ca versus the scaled excess energy. Experimental data are depicted with open black circles and the CCC calculations (HF, velocity gauge) with closed blue circles. The line styles of the best fits to our data are the same as in figure 1. The fit with the analytical shape function of Pattard (see text) is shown by green dot-dashed lines. The thick solid magenta line represents the scaled LOPT calculations of Mikhailov *et al.* [7].

potential E^+, calculated with the GRASP code [24], the asymptotic SO ratios from [34] and for He-like targets also the DPI threshold energies E^{2+} were kept fixed in the fitting procedure. The results of best fits to Al and Si data are depicted in figure 1. Indeed, the KO terms of He-like ions multiplied by the Z^4/Z^{*4} ratios are close in magnitude to the ones for neutral atoms. The effective nuclear charge Z^* was deduced using the hydrogenic formula $E^+=Z^{*2}Ry$, where Ry = 13.6 eV, and for the He-like targets $Z^*=Z$. These results suggest that KO dominates near threshold and for intermediate excitation energies.

The experimental and theoretical CCC double-to-single photoionization cross-secions of Mg and Ca versus the reduced excess energy are presented in figure 2. The two sets of data were also fitted with our empirical SO-KO model. It can be seen that for Mg the overall shape and magnitude of CCC calculations is in excellent agreement with the experimental P_{KK} values, while for Ca the calculations underestimate the experimental data. For both Mg and Ca, a relative shift of the CCC curves towards the $(E-E^{2+})/Z^{*2}$ value for two-electron targets can be observed. For comparison, the predictions within the lowest-order perturbation theory (LOPT) by Mikhailov *et al.* [7] are also depicted in figure 2. The plotted LOPT curves were obtained by scaling the suggested universal ratio of the double-to-single K-shell photoionization cross-sections for neutral atoms from Ref. [7]. Note, that Mikhailov *et al.* deduce the effective nuclear charge Z^* from the first ionization potential (K-shell binding energy) and not E^+. The LOPT curves are found to be quite close to the CCC calculations for Mg, and slightly lower to those for Ca.

It also instructive to fit the data with the universal shape function for single-photon multiple ionization proposed by Pattard [35]:

$$\frac{\sigma^{2+}}{\sigma^{+}} = R_\infty \frac{E^\alpha (\Delta E + E_0)^{7/2}}{(\Delta E + E_1)^{\alpha+7/2}}, \qquad (1)$$

where ΔE is the excess energy, α stands for the Wannier threshold exponent (α varies smoothly from 1.056 (Z=2) to 1.0 in the limit $Z\rightarrow\infty$), R_∞ is the asymptotic double-to-single photoabsorption ratio, and E_0 and E_1 are fit parameters. This shape function is based on the proposed analytical parametrization for ionization by bare projectiles [36], and it satisfies the Wannier law near threshold and the Bethe-Born theory at high-energies. The fitted curves for

Mg and Ca are shown as dot-dashed lines in figure 2. In the fitting procedure R_∞ was fixed at values from Ref. [34]. While for He-like ions $E_0 \approx 2E_1$, the E_0 paramaters were found to be $\sim 2.5E_1$ for the experimental P_{KK} of Mg, Al and Si and $\sim 2.7E_1$ for Ca, respectively. The fits to CCC calculations yield $\sim 2.4E_1$ for both Mg and Ca. These values are in contrast with the ones reported by Huotari *et al.* [11] who find E_0 almost equal to E_1. Indeed, only when letting R_∞ free in the fit we find $E_0 \sim E_1$, but then R_∞ takes the value of $\sim P_{KK}^{max}$. On inspection of figure 2 it can be seen that the fit with the universal shape function by Pattard works quite well for both the measured data and the CCC calculations, and is comparable to the curves from the SO-KO model fit.

4.2. Scaling laws

It is worthwhile to ask whether the scaling properties of DPI cross sections and the double-to-single photoionization cross-section ratios for two-electron systems suggested by Kornberg and Miraglia [37], hold for neutral atoms. To this end, first power-law fits to the maximum values of σ^{2+} as a function of Z^* were performed. As expected, for He-like ions a $Z^{*-4.08(3)}$ fall-off was found, however, for neutral atoms a $Z^{*-3.68(11)}$ dependence was determined (see figure 3b). Indeed, the scaled double photoionization cross sections for Mg, Al, Si and Ca in reduced coordinates $\sigma^{2+}Z^{*3.68}$ against $(E\text{-}E^{2+})/Z^{*2}$ collapse onto a single curve (see figure 3a). Further, the $\sigma^{2+}Z^{*3.68}$ data for neutral atoms in the range $2 \leq Z \leq 47$, within the experimental uncertainties, exhibit a universal scaling behavior and coincide with the $\sigma^{2+}Z^{*4}$ for the He isoelectronic series. A hint to the difference for the scaling exponents of σ^{2+} is already given in

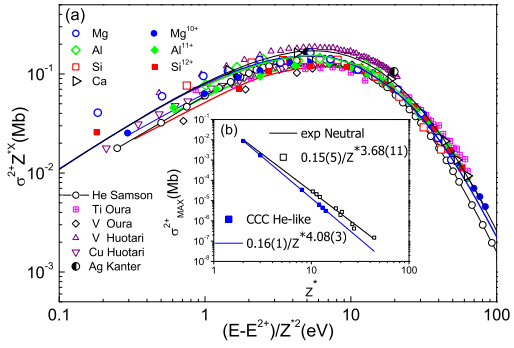

Figure 3. (a) Scaled experimental DPI cross sections for Mg, Al, Si and Ca compared to the scaled CCC calculations for He-like ions and experimental data for higher Z elements as a function of the scaled excess energy. The curves were deduced from the fitted values of P_{KK}. (b) Shown are the power-law fits to the maximum values of σ^{2+} as a function of Z^*.

the weaker Z dependence of P_{KK}^{max} for neutral atoms of $Z^{-1.61(5)}$ [10, 12]. In this perspective, one should not expect the double-to-single photoionization cross-section ratios for neutral atoms to obey the scaling relation with Z^{*2} which is valid for the He-isoelectronic sequence [3]. Indeed, figure 4 illustrates that the scaled double-to-single photoionization cross-section ratios for neutral elements do not fall on one curve.

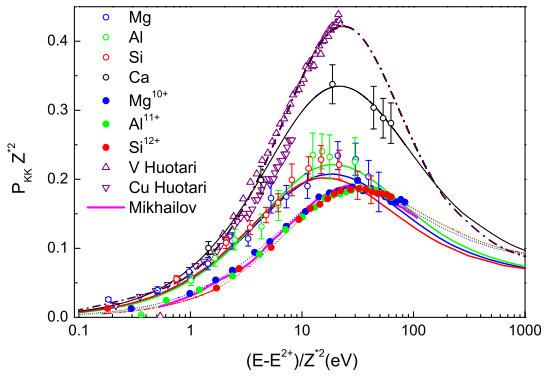

Figure 4. Scaled double-to-single photoionization cross-section ratios versus the scaled excess energy. The curves represent the fit with the SO-KO model. Solid lines correspond to our experimental results and dashed lines to CCC calculations for He-like ions, respectively. Experimental data for V and Cu are from Huotari *et al.* [11], where the dot-dashed line shows the fit with Pattard's shape function. The thick solid magenta line represents the calculations of Mikhailov *et al.* [7].

5. Concluding Remarks

The comparison of our results with other experimental data and CCC calculations suggest that the *post*-photoabsorption electron-electron correlation is different for neutral atoms and He-like ions. An empirical model to separate the knock-out (KO) and shake-off (SO) mechanisms of the K-shell DPI process is proposed. It was demonstrated that the K-shell double-to-single photoionization cross-section ratios of neutral atoms do not obey the Z^{*2} scaling. A semiempirical universal scaling of the double photoionization cross sections with the effective nuclear charge for neutral atoms in the range $2 \leq Z \leq 47$ was established.

Acknowledgments

The support of the Swiss National Science Foundation and the ESRF is acknowledged. Resources of the National Computational Infrastructure (NCI) Facility were used.

References

[1] Hino K, Hino K I, Ishihara T, Shimizu F, Toshima N and McGuire J H 1993 *Phys. Rev. A* **48** 1271
[2] Schneider T, Chocian P L and Rost J M 2002 *Phys. Rev. Lett.* **89** 073002
[3] Schneider T and Rost J M 2003 *Phys. Rev. A* **67** 062704
[4] Kheifets A S 2001 *J. Phys. B: At. Mol. Opt. Phys.* **34** L247
[5] Briggs J S and Schmidt V 2000 *J. Phys. B: At. Mol. Opt. Phys.* **33** R1
[6] Avaldi L and Heutz A 2005 *J. Phys. B: At. Mol. Opt. Phys.* **38** S861
[7] Mikhailov A I, Mikhailov I A, Moskalev A N, Nefiodov A V, Plunien G and Soff G 2004 *Phys. Rev. A* **69** 032703
[8] Colgan J, Pindzola M S and Robicheaux F 2001 *J. Phys. B: At. Mol. Opt. Phys.* **34** L457
[9] Knapp A *et al.* 2002 *Phys. Rev. Lett.* **89** 033004
[10] Kanter E P, Ahmad I, Dunford R W, Gemmell D S, Krässig B, Southworth S H and Young L 2006 *Phys. Rev. A* **73** 022708
[11] Huotari S, Hämäläinen K, Diamant R, Sharon R, Kao C C and Deutsch M 2008 *Phys. Rev. Lett.* **101** 043001
[12] Kanter E P, Dunford R W, Krässig B and Southworth S H 1999 *Phys. Rev. Lett.* **83** 508
[13] Southworth S H, Kanter E P, Krässig B, Young L, Armen G B, Levin J C, Ederer D L and Chen M H 2003 *Phys. Rev. A* **67** 062712
[14] Oura M *et al.* 2002 *J. Phys. B: At. Mol. Opt. Phys.* **35** 3847
[15] Diamant R, Huotari S, Hämäläinen K, Sharon R, Kao C C and Deutsch M 2009 *Phys. Rev. A.* **79** 062511
[16] Diamant R, Huotari S, Hämäläinen K, Sharon R, Kao C C, Honkimäki V, Buslaps T and Deutsch M 2009 *Phys. Rev. A.* **79** 062512
[17] Hoszowska J *et al.* 2009 *Phys. Rev. Lett.* **102** 073006
[18] Kheifets A S, Bray I and Hoszowska J 2009 *Phys. Rev. A* **79** 042504
[19] Samson J A R, Stolte W C, He Z X, Cutler J N, Lu Y and Bartlett R J 1998 *Phys. Rev. A* **57** 1906
[20] Hoszowska J, Dousse J Cl, Kern J and Rhême Ch 1996 *Nucl. Instr. Meth. Phys. Res. A* **376** 129
[21] Chen M H 1991 *Phys. Rev. A* **44** 239
[22] http:/physics.nist.gov/xcom
[23] Hart J F and Herzberg G 1957 *Phys. Rev.* **106** 79
[24] Dyall K G, Grant I P, Johnson C T, Parpia F A and Plummer E P 1989 *Comp. Phys. Comm.* **55** 425
[25] Kheifets A S and Bray I 1998 *Phys. Rev. A* **57** 2590
[26] Kheifets A S and Bray I 1998 *Phys. Rev. A* **58** 4501
[27] Kheifets A S and Bray I 2007 *Phys. Rev. A* **75** 042703
[28] Samson J A R 1990 *Phys. Rev. Lett.* **65** 2861
[29] Pattard T and Burgdörfer J 2001 *Phys. Rev. A* **64** 042720
[30] Pattard T, Schneider T and Rost J M 2003 *J. Phys. B: At. Mol. Opt. Phys.* **36** L189
[31] Mitnik D M and Miraglia J 2005 *J. Phys. B: At. Mol. Opt. Phys.* **38** 3325
[32] Aichele K *et al.* 1998 *J. Phys. B: At. Mol. Opt. Phys.* **31** 2369
[33] Thomas T D 1984 *Phys. Rev. Lett.* **52** 417
[34] Forrey R C, Sadeghpour H R, Baker J D, III J D M and Dalgarno A 1995 *Phys. Rev. A* **51** 2112
[35] Pattard T 2002 *J. Phys. B: At. Mol. Opt. Phys.* **35** L207
[36] Rost J M and Pattard T 1997 *Phys. Rev. A* **55** R5
[37] Kornberg M A and Miraglia J E 1994 *Phys. Rev. A* **49** 5120